CORA Cork Open Research Archive
Cartlann Taighde Oscailte Chorcaí

Title	Extracting filtered signal statistics of continuously measured quantum systems
Authors	Kiely, Anthony;Landi, Gabriel
Publication date	2026-03-25
Original Citation	Kiely, A & Landi, G 2026, 'Extracting filtered signal statistics of continuously measured quantum systems', Physical Review A, vol. 113, no. 3, 032442, pp. 1-12. https://doi.org/10.1103/yxqg-93jz
Type of publication	Article (peer-reviewed)
Link to publisher's version	https://www.scopus.com/pages/publications/105036632950 - 10.1103/yxqg-93jzhttps://www.scopus.com/pages/publications/105036632950?origin=resultslist
Rights	© 2026, the Authors. Published by the American Physical Society under the terms of the Creative Commons Attribution 4.0 International license. Further distribution of this work must maintain attribution to the author(s) and the published article's title, journal citation, and DOI. - https://creativecommons.org/licenses/by/4.0/
Download date	2026-10-10 18:04:04
Item downloaded from	https://hdl.handle.net/10468/18937

UCC
University College Cork, Ireland
Coláiste na hOllscoile Corcaigh

Extracting filtered signal statistics of continuously measured quantum systems

Anthony Kiely [1,2,3,*] and Gabriel Landi [4,5]

[1]*School of Physics, University College Dublin, Belfield, Dublin 4, Ireland*
[2]*Centre for Quantum Engineering, Science, and Technology, University College Dublin, Belfield, Dublin 4, Ireland*
[3]*School of Physics, University College Cork, College Road, Cork, Ireland*
[4]*Department of Physics and Astronomy, University of Rochester, Rochester, New York 14627, USA*
[5]*Center for Coherence and Quantum Science, University of Rochester, Rochester, New York 14627, USA*

(Received 14 July 2025; accepted 9 March 2026; published 25 March 2026)

The joint state of a continuously monitored quantum system and the classical filtered measurement record has recently been shown to be described by a quantum Fokker-Planck master equation [Phys. Rev. Lett. **129**, 050401 (2022)]. We present a deterministic approach to compute the steady state of the system and detector. The method is shown to become particularly efficient in the absence of feedback, which we exploit to develop a perturbative approach valid for weak feedback. We show that through this method we can extract the full counting statistics of the signal, the quantum-classical mutual information between the system and signal, and the Fisher information of the signal, which can be used for sensing applications. Our results are illustrated with both single-qubit models and the spin chains governed by the one-dimensional transverse field Ising model or the Lipkin-Meshkov-Glick model.

DOI: 10.1103/yxqg-93jz

I. INTRODUCTION

In contrast with textbook instantaneous projective measurements, continuous measurements allow one to extract partial information about a quantum state without fully collapsing it [1]. In addition, continuous measurements allow for the implementation of feedback protocols, where the classical (noisy) data obtained from the measurements are fed back in real time to the system. Quantum continuous measurements have been experimentally realized across many quantum platforms, such as optical cavities [2], quantum dots [3,4], and superconducting circuits [5–7].

The inclusion of feedback makes the dynamics nonlinear and time nonlocal, dramatically complicating any theoretical description. Feedback schemes can be simulated numerically using stochastic trajectories; however, deterministic descriptions remain extremely valuable. This is tantamount to the distinction between the Langevin equation and the Fokker-Planck equation in Brownian motion. The two descriptions are complementary. Both describe the same physical process, but from different perspectives. For quantum continuous measurements a similar distinction exists. In the absence of feedback, the analog of the Fokker-Planck equation, i.e., the deterministic evolution, is simply the quantum master equation. However, in the presence of feedback this is no longer true. For this reason, traditionally, such methods have been largely restricted to what is known as current-based feedback, where at each step only the very last data point, called a current $z(t)$, is used to guide the feedback [8]. In this paradigm the current $z(t)$ is a random variable and one could, for example, modify the Hamiltonian based on the obtained value of z at each step. More recently, this has been extended to charge-based feedback [9], where one uses instead the entire integrated current $N(t) = \int_0^t dt' z(t')$.

Both examples are actually particular cases of a low-pass filter-based feedback, where one uses instead

$$D(t) = \int_0^t dt' \gamma e^{-\gamma(t-t')} z(t'), \tag{1}$$

which recovers the current- and charge-resolved cases when $\gamma \to \infty$ and $\gamma \to 0$, respectively. Recently, a deterministic method for simulating feedback based on this kind of low-pass filter was put forward in Ref. [10], for the case of the diffusive unraveling of the master equation. In this formalism, in addition to the usual open system dynamics, an external agent is also continuously measuring a certain operator A through a weak Gaussian measurement defined by Kraus operators

$$K(z) = \left(\frac{2\lambda dt}{\pi}\right)^{1/4} e^{-\lambda dt (z-A)^2}, \tag{2}$$

with strength λ. In the limit of infinite measurement strength, this reduces to projective measurements of A. Reference [10] introduced a signal-resolved density matrix $\rho_t(D)$, defined such that $\mathrm{Tr}[\rho_t(D)] = P(D)$ equals the probability that the signal has a certain value D at time t. This mathematical object $\rho_t(D)$ can be thought of as the joint (quantum-classical) state of the quantum system and the classical measurement

*Contact author: AKiely@ucc.ie

Published by the American Physical Society under the terms of the Creative Commons Attribution 4.0 International license. Further distribution of this work must maintain attribution to the author(s) and the published article's title, journal citation, and DOI.

apparatus. Their main result was to show that $\rho_t(D)$ satisfies a Fokker-Planck master equation of the form

$$\partial_t \rho_t(D) = \mathcal{L}(D)\rho_t(D) + \lambda \mathcal{D}[A]\rho_t(D) - \gamma\, \partial_D \mathcal{C}_{A-D}\rho_t(D)/2 + \frac{\gamma^2}{8\lambda}\partial_D^2 \rho_t(D), \tag{3}$$

where $\mathcal{L}(D) = \mathcal{L}_0 + \sum_p f_p(D)\mathcal{L}_p$ is the Liouvillian which can in principle have any dependence on the signal D. Here $\mathcal{C}_X = \{X, \cdot\}$ is the anticommutator with X and $\mathcal{D}[A] = A \cdot A^\dagger - \frac{1}{2}\{A^\dagger A, \cdot\}$ is the Lindblad dissipator. Feedback enters through the fact that the Liouvillian $\mathcal{L}(D)$ is allowed to depend on the signal D. Here we assume, without loss of generality, that this dependence enters through a set of functions $f_p(D)$ that couple to Liouvillian terms $\mathcal{L}_p$. This therefore allows for feedback that can be either coherent (i.e., terms that enter into the system Hamiltonian) or incoherent (which enters into, e.g., jump operators). Equation (3) was derived assuming an evolution that combines the natural Liouvillian evolution, with $\mathcal{L}$, as well as the continuous application of Gaussian weak measurements defined by the Kraus operations in Eq. (2). The new terms that appear on the right-hand side of Eq. (3) can be given a specific physical intuition: The second term is the measurement backaction, which leads to dephasing in the basis of the observable A that one is measuring, and the third and fourth terms can be interpreted as analogous to the drift and diffusion terms in the standard Fokker-Planck equation.

This type of master equation has since been used to study the generation of steady-state entanglement from thermal resources using feedback [11], the cooling of a particle in a harmonic trap [12], and the exploration of Maxwell demons in quantum and classical mechanics [13]. Equation (3) has also recently been generalized to the case of multiple detectors [12]. However, actually solving Eq. (3) is not an easy task. It has the structure of a Fokker-Planck equation (linear, second-order parabolic differential equation), but the object itself is a density matrix. So this is akin to a system of coupled Fokker-Planck equations. The starting point of this paper is a solution method briefly proposed in the Supplemental Material of Ref. [10]. Our first main result is the realization that, in the absence of feedback, this method can be modified to become extremely simple and efficient to use. It allows access to the full counting statistics of the signal $D(t)$ [Eq. (1)], including all statistical moments and the full probability density function $P_t(D)$. It also gives access to measures of correlation between system and signal, namely, the mutual information between $D(t)$ and the quantum state of the system, as well as any correlation function between $D(t)$ and a system observable. Finally, it gives access to the Fisher information contained in the signal, which is relevant when $D(t)$ is used for sensing applications. All of these results concern Eq. (3) in the absence of feedback. We then move on to show that they can be extended to the case of weak feedback, using a perturbative approach which we develop. Taken together, our results therefore provide a comprehensive toolbox for efficiently extracting results from Eq. (3). A brief comparison with stochastic simulations of quantum trajectories is provided in Appendix A.

II. FORMAL FRAMEWORK

Our starting point is a solution method of Eq. (3) that was put forward in Ref. [10]. It consists in expanding the density operator in terms of a complete basis of generalized Hermite polynomials

$$\rho_t(D) = \sum_{n=0}^{\infty} M_n \frac{\mathcal{H}_n(D)}{\sqrt{\sigma^n n!}} \frac{e^{-D^2/2\sigma}}{\sqrt{2\pi\sigma}}, \tag{4}$$

with

$$\mathcal{H}_n(x) = \left(\frac{\sigma}{2}\right)^{n/2} H_n\left(\frac{x}{\sqrt{2\sigma}}\right), \tag{5}$$

where $\mathcal{H}_n(x)$ are generalized Hermite polynomials, $H_n(x)$ are standard physicist's Hermite polynomials, and M_n are Hermitian matrices of dimension R. Here we also define the diffusion coefficient

$$\sigma = \frac{\gamma}{8\lambda}. \tag{6}$$

This choice of ansatz is motivated by the eigenfunctions of the drift and diffusion part of Eq. (3). It means that we can fully describe the signal-resolved state $\rho_t(D)$ in terms of the set of matrices M_n. In principle, we need to consider all M_n from $n = 0$ to ∞, but, in practice, as shown below, the sum (4) can be truncated to a total of N terms, where N simply needs to be large enough to ensure convergence. In the majority of the examples presented, a value of $N \approx 100$ is found to be sufficient. For sufficiently large N, any state can be represented by this choice of ansatz. The methods for actually extracting M_n will be discussed starting in Sec. III. In the remainder of this section, we assume that the M_n are known and we show what kind of information can be extracted from them. We note in particular that for various quantities of interest only a handful of the M_n matrices are actually needed.

A. Statistics of $D(t)$

We start by defining the coefficients

$$c_m = \mathrm{Tr}(M_m) = \int dD\, P(D) \frac{\mathcal{H}_m(D)}{\sqrt{\sigma^m m!}}. \tag{7}$$

Note that $c_0 = 1$. The full distribution of the signal outcomes is obtained from Eq. (4) as

$$P_t(D) = \mathrm{Tr}[\rho_t(D)] = \sum_{n=0}^{\infty} c_n \frac{\mathcal{H}_n(D)}{\sqrt{\sigma^n n!}} \frac{e^{-D^2/2\sigma}}{\sqrt{2\pi\sigma}}. \tag{8}$$

From this one can construct the statistical moments of the signal

$$\langle D^n \rangle(t) = \int dD P_t(D) D^n. \tag{9}$$

This is an ensemble expectation, i.e., taken over the ensemble of measurement outcomes. It can therefore be evaluated at any instant of time or in steady state. Due to the orthogonality of the Hermite polynomials, the average of $P_t(D)$ is

$$\langle D \rangle = \sqrt{\sigma} c_1. \tag{10}$$

Thus, if all one is interested in is the average, it suffices to know M_0 and M_1 only. Similarly, the second moment

$\langle D^2\rangle = \sqrt{2}\sigma c_2 + \sigma$. This gives the variance as

$$\mathrm{Var}(D) = \sigma\left(1 + \sqrt{2}c_2 - c_1^2\right). \tag{11}$$

More generally, the qth moment is

$$\langle D^q\rangle = \sum_n c_n J_n(q), \quad J_n(q) = \int dD\, D^q \frac{\mathcal{H}_n(D)}{\sqrt{\sigma^n n!}} \frac{e^{-D^2/2\sigma}}{\sqrt{2\pi\sigma}}. \tag{12}$$

This integral can be solved recursively using

$$J_n(q) = \sqrt{\sigma(n+1)}J_{n+1}(q-1) + \sqrt{n\sigma}J_{n-1}(q-1), \tag{13}$$

$$J_n(0) = \delta_{n,0}. \tag{14}$$

Since $J_n(q)$ is only nonzero for $n \leqslant q$, only the first $q+1$ coefficients are needed to compute $\langle D^q\rangle$. Thus, to compute $\langle D^q\rangle$ we only need to know $M_0, \ldots, M_q$.

The characteristic function of $P_t(D)$ can also be constructed from the coefficients c_n as

$$\langle e^{iKD}\rangle = e^{-K^2\sigma/2} \sum_{n=0}^{\infty} c_n \frac{(iK)^n \sigma^{n/2}}{\sqrt{n!}}. \tag{15}$$

From this we can then reconstruct $P_t(D)$ by taking the inverse Fourier transform. In practice, we have found this to be quite useful, since a direct reconstruction using Eq. (8) leads to poor convergence due to fast oscillating terms. With the characteristic function $\langle e^{iKD}\rangle$, we can first filter out very high frequencies and then take the inverse Fourier transform.

B. Quantum-classical correlations between system and detector

The joint state of the system allows one to determine the correlations between the detector outcomes and the quantum system. First, one may define the quantum-classical mutual information between system and detector as

$$\mathcal{I}(t) = S\left[\int dD \rho_t(D)\right] + S[\mathrm{Tr}[\rho_t(D)]] - S[\rho_t(D)], \tag{16}$$

where $S[\cdot]$ is either the von Neumann or Shannon entropy, depending on the input. This can be simplified (see Appendix B) as

$$\mathcal{I}(t) = -\int dD\, S[\tilde{\rho}_t(D)]P(D) + S[M_0], \tag{17}$$

where $\tilde{\rho}_t(D) = \rho_t(D)/P(D)$ is the conditional state of the system given an outcome D. Equation (17) is a positive quantity, with a maximum value $\ln R$, where R is the dimension of the Hilbert space of the system. Low values of $\mathcal{I}$ indicate that the system and detector are roughly statistically independent, while very high values correspond to a detector signal which is very informative about the system state.

In general, computing $\mathcal{I}$ requires many matrices M_n for convergence. A comparatively simpler quantity to calculate is the covariance between the signal and a particular system observable B, defined as

$$\mathrm{cov}_t(B, D) = \int dD\, D\, \mathrm{Tr}[B\rho_t(D)] - \langle D\rangle\langle B\rangle \tag{18}$$

$$= \sqrt{\sigma}[\mathrm{Tr}(M_1 B) - \mathrm{Tr}(M_1)\mathrm{Tr}(M_0 B)]. \tag{19}$$

In (19) (derived in Appendix B) we have shown how this can be computed using only M_0 and M_1. Intuitively, $\mathrm{cov}(B, D)$ provides a measure of the correlation between the quantum state in the basis of the observable B and the continuous filtered measurement outcome D. Note that the usual quantum mutual information is lower bounded by the corresponding covariance [14], motivating us to consider the analogous pair of objects in the context of continuous monitoring.

C. Two-time correlation and Fisher information of steady-state filtered output current

The quantities described above can be determined solely from knowledge of the matrices M_n, in cases with or without feedback. In this section we describe two other quantities of interest, whose calculation is somewhat more complicated. In particular, we have only been able to find explicit formulas for them in the case of no feedback. Their actual computation is done in Sec. III A. Equation (18) is an equal-time correlation function. One can also be interested in two-time correlation functions. The two-time function of the signal is defined as

$$C(t, \tau) = \langle D(t+\tau)D(t)\rangle - \langle D(t)\rangle^2. \tag{20}$$

In Eq. (36) below and Appendix C, we provide an explicit formula for this quantity in the case of no feedback and in the steady state [for which $C(t, \tau)$ is a function only of τ].

Next we turn to the Fisher information. Let μ denote any parameter that appears in Eq. (3). This could be some term in the Hamiltonian or some jump operator. The probability distribution $P_t(D)$ contains information about μ. Therefore, measurements of D can be used to estimate μ. The Fisher information represents the total information about μ that is contained in $P_t(D)$ and is defined as

$$F_\mu = \int dD \frac{[\partial_\mu P_t(D)]^2}{P_t(D)}. \tag{21}$$

The Fisher information lower bounds the variance of the estimated parameter μ via the Cramér-Rao bound [15,16]. We note that F_μ refers to the classical Fisher information of the empirical distribution [17], where the temporal correlations are discounted, i.e., readings are collated to build a histogram for $P(D)$ in steady state. In practice, we must compute the Fisher information at some fixed value of the parameter. The numerical computation of $\partial_\mu P_\mu(D)$ will be addressed in the next section, for the setting of the no-feedback steady state.

III. EVOLUTION EQUATION FOR M_n

The results in the preceding section are all based on the decomposition (4) of the signal-resolved density matrix, which is defined by the set of matrices M_n. We now turn to the question of how to actually compute these M_n, which is based on the method proposed in [10]. We start by using the decomposition $\mathcal{L}(D) = \mathcal{L}_0 + \sum_p f_p(D)\mathcal{L}_p$ of the Liouvillian, into the feedback-independent part $\mathcal{L}_0$ and the feedback terms $\mathcal{L}_p$. Inserting Eq. (4) in Eq. (3) yields a system of coupled equations for the operators M_n (see Appendix D for more

details),

$$\dot{M}_m = \mathcal{L}_0 M_m + \sum_{n=0}^{N-1}\sum_p \alpha_{n,m,p}\mathcal{L}_p M_n - \frac{\lambda}{2}[A,[A,M_m]] - \frac{\gamma}{2}\left(2mM_m - \sqrt{\frac{m}{\sigma}}\{A, M_{m-1}\}\right), \tag{22}$$

where

$$\alpha_{n,m,p} = \int_{-\infty}^{\infty} dD \frac{\mathcal{H}_m(D)}{\sqrt{\sigma^m m!}}\frac{\mathcal{H}_n(D)}{\sqrt{\sigma^n n!}}\frac{e^{-D^2/2\sigma}}{\sqrt{2\pi\sigma}} f_p(D) \tag{23}$$

are coefficients determined by the feedback functions $f_p(D)$. For example, in the case of a Heaviside step function $f_p(D) = \theta(D)$, these coefficients become [10]

$$\alpha_{n,m,p} = \begin{cases} 1/2 & \text{for } n = m \\ 0 & \text{for } n+m \text{ even} \\ \frac{(-1)^{(n+m-1)/2} m!!(n-1)!!}{\sqrt{2\pi n! m!}(m-n)} & \text{for } n+m \text{ odd.} \end{cases} \tag{24}$$

Similarly, in the case of linear feedback $f_p(D) = D$ we get

$$\alpha_{n,m,p} = \sqrt{\sigma}(\sqrt{n+1}\delta_{m-1,n} + \sqrt{n}\delta_{m+1,n}). \tag{25}$$

The matrix elements can be computed analytically for any case where $f_p(D)$ is polynomial in D using recursive relations, as summarized in Appendix E.

Equation (22) can be written more compactly as a single vector equation. We truncate the infinite sum in Eq. (4) to a sufficiently large N and define a vector of matrices $\vec{M} = (M_0 M_1 M_2 \cdots M_{N-1})^T$. Our dynamical equation can now be succinctly expressed as

$$\partial_t \vec{M} = \hat{Q}\vec{M}, \tag{26}$$

where $\hat{Q} = \hat{Q}_0 + \hat{Q}_{\text{fb}}$ with

$$\hat{Q}_0 = 1_N \otimes \mathcal{L}_0 + \lambda 1_N \otimes \mathcal{D}[A] - \gamma F \otimes 1_d + \frac{\gamma}{2\sqrt{\sigma}} G \otimes \mathcal{C}_A,$$

$$\hat{Q}_{\text{fb}} = \sum_p \alpha_p \otimes \mathcal{L}_p. \tag{27}$$

Here 1_x is the identity operator of dimension x, whereas F, G, and α_p are $N \times N$ matrices with elements

$$F = \text{diag}(0, 1, 2, \ldots, N-1), \tag{28}$$

$$[G]_{n,m} = \sqrt{j}\delta_{n,m+1}, \tag{29}$$

$$[\alpha_p]_{n,m} = \alpha_{n,m,p}. \tag{30}$$

The system Hilbert space has dimension R, so the Liouvillian has dimension $d = R^2$. The total dimension of the matrix $\hat{Q}$ is then $R^2 N$.

A. Case of no feedback

The challenging aspect of Eq. (22), or its more compact version (26), is that they involve a set of coupled equations for all the matrices M_m which must therefore be solved simultaneously. An interesting realization, however, is that the entire result simplifies dramatically if there is no feedback, that is, if all functions $f_p(D) \equiv 0$. This implies the matrices $\alpha_p = 0$ vanish, and so only $\hat{Q}_0$ contributes to Eq. (26). This operator, however, has the very special property of being block lower triangular, which means that each M_m depends only on the previous one. For the steady-state solution ($\dot{M}_m = 0$), all of the matrices can therefore be solved using forward substitution. More specifically, we first solve for M_0 and then we insert this into the equation for $m = 1$ and solve for M_1. This in turn is inserted into the equation for $m = 2$, which yields M_2. This can then be continued in an iterative fashion. This matches well with the fact, discussed in the previous section, that various quantities of interest only require a handful of M_m. The equation for M_0 becomes

$$\Lambda M_0 = 0, \quad \Lambda := \mathcal{L}_0 + \lambda\mathcal{D}[A], \tag{31}$$

which is simply the usual steady-state solution for the unconditional dynamics, with Liouvillian Λ. From M_0 one can then recursively solve for the other terms using

$$(\Lambda - \gamma n 1_d)M_n = -\frac{\gamma}{2}\sqrt{\frac{n}{\sigma}}\mathcal{C}_A(M_{n-1}) \tag{32}$$

for $n = 1, 2, \ldots$. Note that, provided there is a unique solution for M_0, this solution is uniquely determined. This iterative process can also be made faster by first finding the spectrum of the unconditional Liouvillian

$$\Lambda = \sum_{j\neq 0} \eta_j |x_j)(y_j|, \tag{33}$$

where $|x_j)$ and $(y_j|$ are the right and left eigenvectors associated with eigenvalue η_j. Specifically, $|x_0) = |M_0)$, $(y_0| = (1_d|$, and $\eta_0 = 0$. Even though a Liouvillian itself is not invertible, the quantity $\Lambda - \gamma n 1_d$ will be, for any $n \neq 0$. In fact, from the eigenspectrum on readily finds

$$(\Lambda - \gamma n 1_d)^{-1} = \sum_{j\neq 0}(\eta_j - \gamma n)^{-1}|x_j)(y_j| - \frac{1}{\gamma n}|M_0)(1_d|. \tag{34}$$

The recursion relation can then be expressed as

$$|M_n) = -\frac{\gamma}{2}\sqrt{\frac{n}{\sigma}}\sum_{j=0}\frac{(y_j|\mathcal{C}_A|M_{n-1})}{\eta_j - \gamma n}|x_j). \tag{35}$$

This same decomposition also allows one to compute the correlations in the measurement current (see Appendix C),

$$C(\tau) = \langle D(t+\tau)D(t)\rangle - \langle D(t)\rangle^2 \tag{36}$$

$$= \sigma e^{-\gamma\tau} + \frac{1}{2}\sum_{j\neq 0}\frac{\gamma(\gamma e^{\tau\eta_j} + e^{-\gamma\tau}\eta_j)}{\gamma^2 - \eta_j^2}$$

$$\text{Tr}(Ax_j)\text{Tr}(y_j^\dagger\{A, M_0\}). \tag{37}$$

Since the measurement current is typically highly correlated in time, this measure of the fluctuations provides information not accessible from the average (see, for example, [1]). This is also a highly accessible quantity experimentally.

Finally, we can also exploit the recursive nature of Eq. (32) to obtain an expression for evaluating the derivative $\partial_\mu P_t(D)$ of the signal probability distribution with respect to an arbitrary parameter μ appearing in Eq. (3). This quantity is necessary to compute the Fisher information defined in Eq. (21). A straightforward method for computing $\partial_\mu P_t(D)$ is to solve for $P_t(D)$ for a certain value μ and a nearby

value $\mu + \delta\mu$, from which $\partial_\mu P_t(D)$ can then be computed numerically using finite differences. However, $\delta\mu$ must be sufficiently small for the derivative to be well approximated numerically, but not so small as to become comparable to the other numerical errors in the procedure. Due to this nontrivial interplay, we have actually found this method to be numerically quite inaccurate. Instead, we now provide another method, which we have found to be quite efficient, since it completely avoids finite differences. It only works in the absence of feedback and in the steady state. In addition, it assumes that μ is neither λ nor γ. From Eqs. (7) and (8) it follows that

$$\partial_\mu P_t(D) = \sum_{n=0}^{\infty} \mathrm{Tr}(\partial_\mu M_m) \frac{\mathcal{H}_n(D)}{\sqrt{\sigma^n n!}} \frac{e^{-D^2/2\sigma}}{\sqrt{2\pi\sigma}}. \tag{38}$$

Hence, what we ultimately need is $\partial_\mu M_m$. We start with M_0. Differentiating Eq. (31) with respect to μ yields

$$\Lambda(\partial_\mu M_0) = -(\partial_\mu \mathcal{L}_0) M_0, \tag{39}$$

which can be solved for $\partial_\mu M_0$. To get the next terms, we can use the iterative update rule in Eq. (32). Differentiating both sides with respect to μ provides the modified update rule

$$(\Lambda - \gamma n 1_d)(\partial_\mu M_n) = -(\partial_\mu \mathcal{L}_0) M_n - \frac{\gamma}{2}\sqrt{\frac{n}{\sigma}}\mathcal{C}_A(\partial_\mu M_{n-1}), \tag{40}$$

so given $\mathcal{L}_0$, $\partial_\mu M_{n-1}$, and M_n we can once again iteratively solve for $\partial_\mu M_n$. This method is simple to implement because the derivative $\partial_\mu \mathcal{L}_0$ is simple to calculate analytically.

All of the results in this section assume no feedback. At first this might seem to defeat the entire point, since Eq. (3) was actually derived precisely to describe feedback. However, we note two important points. First, as we show next, the results in this section can actually be used as the starting point for a perturbative solution in the case when the feedback is weak. This is a strong motivation in itself. Second, the case of no feedback is actually still of interest, since this is precisely what is studied in the field of full counting statistics [1]. The only new ingredient is the presence of a low-pass filter, which is reasonable from an experimental point of view. This can also be removed, i.e., in the limit $\gamma \to 0$ the expressions presented in this section recover the standard results of full counting statistics [1]. Quantities such as the signal distribution $P_t(D)$ are therefore still valuable and interesting, even in the absence of feedback.

B. Perturbative solution for weak feedback

In the case of feedback, one must solve the full equation (26) for the vector of matrices $\vec{M}$. However, because the dynamical matrix $\hat{Q}$ does not have the block lower triangular structure of $\hat{Q}_0$, the previous approach based on forward substitution cannot be applied. Instead, one must solve for the entire $\vec{M}$ at once, which is computationally much more costly. The situation simplifies, however, if we consider a weak feedback of the form $\hat{Q} = \hat{Q}_0 + \epsilon\hat{Q}_{\mathrm{fb}}$, with $\epsilon \ll 1$. We focus here on the steady state of Eq. (26), which is a solution of

$$\hat{Q}\vec{M} = 0. \tag{41}$$

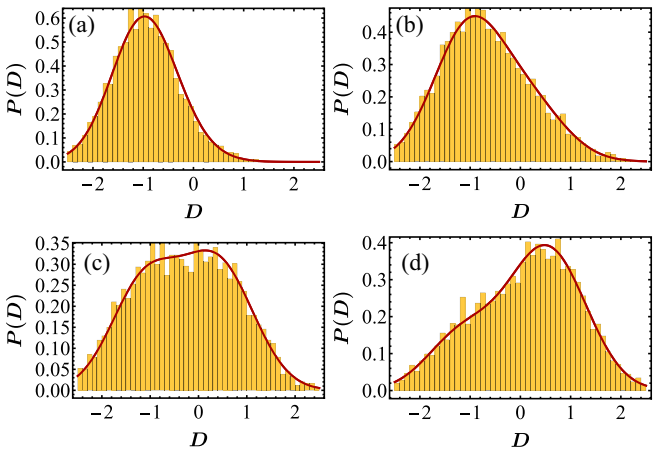

FIG. 1. Measurement outcomes $P(D)$ solving the charge-resolved master equation (red solid line) and collating 5000 stochastic trajectories (orange histograms) for $\Omega = 1$, $\lambda = 0.5$, $\gamma = 2$, and $A = \sigma_z$ at different times (a) $t = \pi/8$, (b) $t = \pi/4$, (c) $t = 3\pi/8$, and (d) $t = \pi/2$.

Series expanding the solution as $\vec{M} \approx \sum_j \epsilon^j \vec{M}^{(j)}$ yields another recursive set of relations

$$\hat{Q}_0\vec{M}^{(0)} = 0, \tag{42}$$

$$\hat{Q}_0\vec{M}^{(j+1)} = -\hat{Q}_{\mathrm{fb}}\vec{M}^{(j)} \tag{43}$$

for $j = 0, 1, 2, \ldots$. More explicitly, what we find is the generalization of Eqs. (31) and (32),

$$\Lambda M_0^{(j+1)} = -(\hat{Q}_{\mathrm{fb}}\vec{M}^{(j)})_0, \tag{44}$$

$$(\Lambda - \gamma n 1_d) M_n^{(j+1)} = -\frac{\gamma}{2}\sqrt{\frac{n}{\sigma}}\mathcal{C}_A\big(M_{n-1}^{(j+1)}\big) - (\hat{Q}_{\mathrm{fb}}\vec{M}^{(j)})_n, \tag{45}$$

with $n = 1, 2, \ldots$ and $j = 0, 1, 2, \ldots$. We first solve these for $j = 0$ and all n up until the truncation N. Then we use these results and solve for all matrices with $j = 1$, and so on, and so forth. Because $\hat{Q}_0$ is lower triangular, solving this system at each iteration is roughly as costly as the case with no feedback.

IV. NUMERICAL EXAMPLES

A. Driven qubit

We illustrate the basic ideas with the simplest Hamiltonian $H = \Omega\sigma_x$ with a measurement $A = \sigma_z$. In Fig. 1 we can see a comparison between the charge-resolved approach in red and the statistical collating of trajectories in the orange histograms. We see good agreement between the two at different times during the Rabi oscillations. A more detailed comparison with the method of stochastic trajectories can be found in Appendix A.

Our approach allows us to analytically calculate the summary statistics of the steady-state probability distribution $P(D)$. In particular, for this example we get that $\langle D\rangle = 0$ and $\mathrm{Var}(D) = \frac{\gamma(\gamma+2\lambda)}{\gamma^2+2\gamma\lambda+4\Omega^2} + \frac{\gamma}{8\lambda}$. The steady-state distribution is shown in Fig. 2. Note that for increasing measurement strength the outcomes become more localized around ± 1,

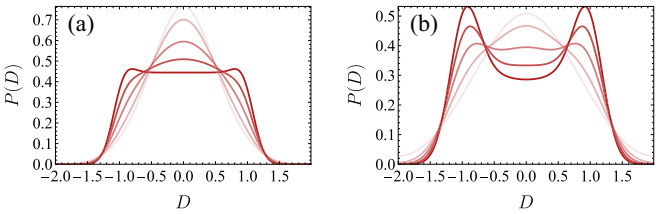

FIG. 2. Steady-state distribution of detector outcomes $P(D)$ for increasing values of measurement strength $\lambda = \{0.5, 1, 1.5, 2, 2.5\}$ for darker shaded lines with measurement bandwidths (a) $\gamma = 0.5$ and (b) $\gamma = 1$.

the eigenvalues of A. The value of γ is associated with the broadening of these peaks.

The dynamical accumulation of correlations between the system and the detector can be seen in Fig. 3(a). The covariance initially grows with time, eventually matching the steady-state value (faded gray lines). The steady-state covariance is also clearly larger for increasing values of measurement strength, which can also be seen in the analytical result,

$$\mathrm{Cov}(\sigma_z) = \frac{\gamma(\gamma + 2\lambda)}{\gamma^2 + 2\gamma\lambda + 4\Omega^2}. \tag{46}$$

The steady-state mutual information is shown in Fig. 3(b), which again increases with increasing measurement strength λ and bandwidth γ. The steady-state covariance for σ_y and σ_z is shown in Figs. 3(c) and 3(d) as a function of measurement strength λ and bandwidth γ. We exclude σ_x since $\mathrm{Cov}(\sigma_x) = 0$. Since the measured observable is $A = \sigma_z$, there is a much higher correlation in the measurement signal and σ_z than σ_y. The $|\mathrm{Cov}(\sigma_z)|$ also increases with both λ and γ.

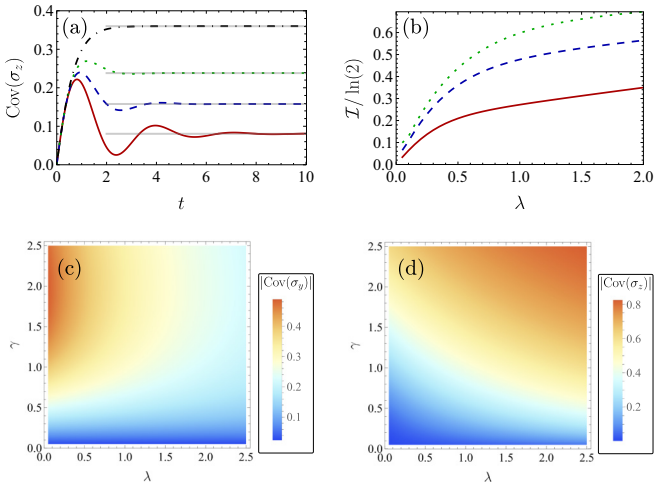

FIG. 3. System detector correlations for the driven qubit. (a) Evolution of $\mathrm{Cov}(\sigma_z)$ with time for $\lambda = \{0.1, 0.5, 1.0, 2.0\}$ (red solid, blue dashed, green dotted, and black dot-dashed lines, respectively). Steady-state values are shown by faded gray lines. (b) Steady-state mutual information $\mathcal{I}$ against measurement strength λ for different bandwidths $\gamma = \{0.5, 1, 1.5\}$ (red solid, blue dashed, and green dotted lines, respectively). (c) Steady-state covariance for σ_y and (d) σ_z. The other parameter values are $\Omega = 1$ and $\gamma = 0.5$.

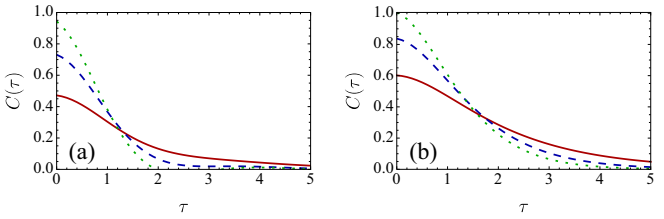

FIG. 4. Two-time correlation function for the measurement current $C(\tau)$ with the parameters $\Omega = 1$ and $\gamma = \{0.6, 1, 1.4\}$(red solid, blue dashed, and green dotted lines, respectively) for measurement strengths (a) $\lambda = 1$ and (b) $\lambda = 1.9$.

The two-time measurement current correlation can also be easily computed in the absence of feedback. For this example, we can see this in Fig. 4. For increasing values of γ, the correlations decay in time more dramatically.

One could also estimate a correction to the known reference Rabi frequency as $H_\mu = (\Omega + \mu)\sigma_x$, which enters as $\mathcal{L}_0^\mu = -i[H_\mu, \cdot]$. In Fig. 5 we show the Fisher information for a range of parameters. First of all, it is clear that for no measurement ($\lambda = 0$), one gets no information $F_\mu = 0$. The Fisher information also vanishes in the limit of very large measurement strength due to the quantum Zeno effect [18] where the dynamics is frozen. Another point worth noting is that the Fisher information decreases with increasing bandwidth γ. This is because a large γ corresponds to the $D(t)$ being the instantaneous measurement outcome, while small γ approaches the case where $D(t)$ is the full integrated current.

B. Multiqubit models

In order to showcase how our method can tackle systems with multiple qubits, we will consider both the Ising and Lipkin-Meskov-Glick (LMG) models.

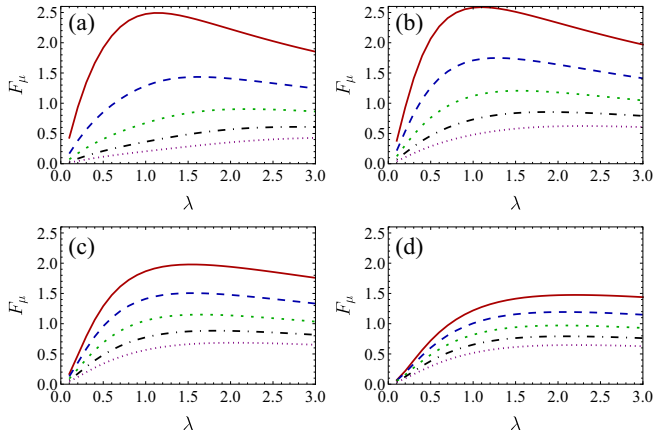

FIG. 5. Fisher information F_μ of the steady-state distribution $P_\mu(D)$ against measurement strength λ for different bandwidths $\gamma = \{0.8, 1, 1.2, 1.4, 1.6\}$ (red solid, blue dashed, green dotted, black dot-dashed, and purple dotted lines, respectively). Each panel shows results for different values of the reference Rabi frequency (a) $\Omega = 0.2$, (b) $\Omega = 0.4$, (c) $\Omega = 0.6$, and (d) $\Omega = 0.8$.

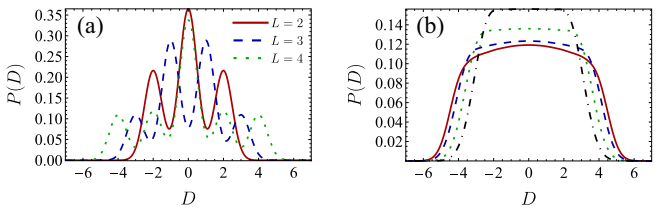

FIG. 6. Steady-state detector probability $P(D)$ for (a) the Ising model for different system sizes L with the parameters $J = 1$, $h = 0.05$, $\lambda = 1$, and $\gamma = 2$ and (b) the LMG model for different values of $h = \{0.1, 1.1, 2.1, 3.1\}$ (red solid, blue dashed, green dotted, and black dot-dashed lines, respectively) with the parameters $L = 4$, $\lambda = 1$, and $\gamma = 3$.

The Ising Hamiltonian is

$$H = J\sum_{j=1}^{L-1}\sigma_{j+1}^{z}\sigma_{j}^{z} + h\sum_{i=1}^{L}\sigma_{i}^{x}, \tag{47}$$

where L is the number of qubits. We will consider a measurement of the total magnetization $A = \sum_{i=1}^{L}\sigma_{i}^{z}$.

We can see the steady-state detector probability $P(D)$ for different system sizes L in Fig. 6(a). Note that the peaks correspond to the eigenvalues of the measured operator A, which explains the structure and broadening of the distribution with increasing system size.

The Hamiltonian for the LMG model can be written in terms of the collective spin operators $S_q = \sum_{i=1}^{L}\sigma_{i}^{q}$ as

$$H = -\frac{1}{L}S_{x}^{2} + hS_{z}. \tag{48}$$

For this model we will consider observable $A = S_y$.

In Fig. 6(b) we show an example of the steady state $P(D)$ for the LMG model for $L = 4$. Note that the large measurement bandwidth relative to the measurement strength leads to a less peaked distribution.

C. Ground-state feedback stabilization

In this final example, we will demonstrate the numerical advantage of the perturbative approach in calculating the feedback dynamics. The setup consists of a single qubit weakly in contact with a thermal bath, described by

$$\mathcal{L}_0 = \kappa n_B\mathcal{D}[\sigma_+] + \kappa(n_B + 1)\mathcal{D}[\sigma_-], \tag{49}$$

where κ is the strength of the coupling and n_B is set by the temperature. The goal is to use feedback control to maintain the qubit in the ground state by correcting for the effects of the bath. The strategy [19,20] is to measure $A = \sigma_x$ and apply a feedback protocol described by $f_1(D) = D$ and $\mathcal{L}_1 = -i[g\sigma_y, \cdot]$. The intuition is that any measured deviation from the ground state is counteracted by this rotation.

In Fig. 7(a) we can see that the feedback control requires sufficient strength g and a short response time $1/\gamma$ to successfully counteract thermalization due to the weakly coupled bath. This is characterized by the ground-state probability $P_0 = \langle 0|M_0|0\rangle$ for the unconditional steady state. In the absence of feedback ($g = 0$), the steady state (including the effects of measurement backaction) has a ground-state population $P_0 \approx 0.505$, which agrees with the results shown.

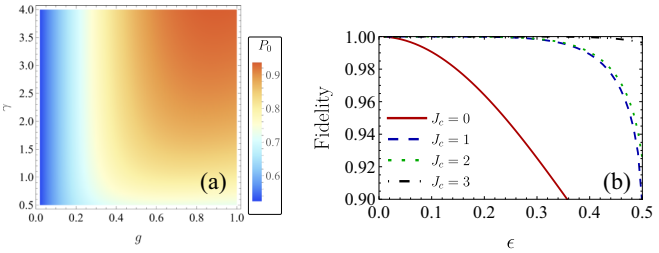

FIG. 7. Ground-state feedback stabilization with measurement strength $\lambda = 0.5$, coupling $\kappa = 0.01$, and temperature $n_B = 0.5$. (a) Steady-state probability for the ground state against feedback strength g and measurement bandwidth γ. (b) Fidelity between unconditional steady states using the exact solution and the perturbative solution with J_c iterations against feedback strength ϵ and $\gamma = 4$.

We now show how our perturbative method can efficiently recreate these results, where g plays the role of ϵ. In Fig. 7(b) we compare the fidelity between the unconditional steady state obtained by exact diagonalization of the full matrix $\hat{Q}$ and using the perturbative method, which has a comparable computational speedup. Higher-order corrections clearly provided increased fidelity with the exact steady-state solution. For $\epsilon = 0.5$, the steady states with and without feedback already differ significantly, while the perturbative solution remains quite close to the exact result.

V. CONCLUSION

In this work we studied feedback control in a continuously monitored quantum system subject to a low-pass filter, as recently derived in Ref. [10]. We explored a solution method based on decomposing the signal-resolved density matrix in a series over Hermite polynomials and showed how this can yield efficient access to various statistical properties of the signal, as well as measures of system-signal correlation. For the particular case of no feedback, we showed how the solution method simplifies dramatically and can be implemented very efficiently. We also illustrated how this could be used as the starting point for a perturbative solution involving weak feedback.

In the setting of open loop quantum control, there is a significant emphasis on both analytical techniques [21] and numerically efficient methods to solve the dynamics which is used to systematically find optimal coherent control pulses [22,23]. Recent efforts in closed loop control have focused on machine learning to determine the optimal feedback control for a specific objective [24,25]. As experimental implementation of continuous weak measurements advances, our approach will aid this with improved numerical efficiency and provide possible perturbative approaches to analytically determine the ideal feedback correction [26].

ACKNOWLEDGMENT

A.K. acknowledges financial support from Taighde Éireann–Research Ireland under Grant No. 24/PATH-S/12701.

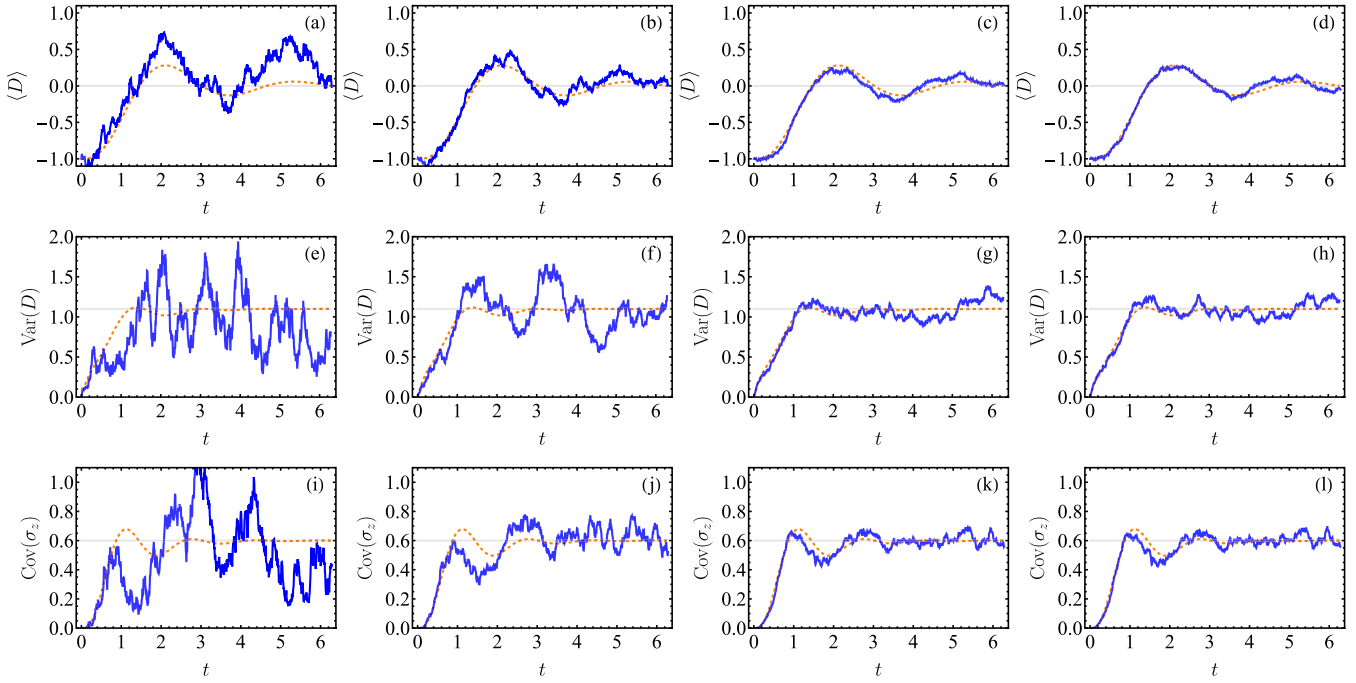

FIG. 8. (a)–(d) Average and (e)–(h) variance of filtered measurement current D, and (i)–(l) covariance $\mathrm{Cov}(\sigma_z, D)$ using stochastic trajectories (blue solid line), the dynamic Fokker-Planck solution (orange dashed line), and the steady-state Fokker-Planck solution (gray horizontal line). The numbers of stochastic trajectories are (a), (e), and (i) 10; (b), (f), and (j) 50; (c), (g), and (k) 250; and (d), (h), and (l) 500. In all panels $N = 5$ and the other parameters are the same as in Fig. 1.

DATA AVAILABILITY

The data that support the findings of this article are not publicly available upon publication because it is not technically feasible and/or the cost of preparing, depositing, and hosting the data would be prohibitive within the terms of this research project. The data are available from the authors upon reasonable request.

APPENDIX A: COMPARISON WITH STOCHASTIC TRAJECTORIES

The standard way to describe a continuously monitored quantum system involves the use of stochastic master equations. For the setting described in the main text, this is the Belavkin equation

$$d\rho_c = \mathcal{L}(D)\rho_c dt + \lambda \mathcal{D}[A]\rho_c dt + \sqrt{\lambda}\{A - \langle A\rangle_c, \rho_c\}dW, \tag{A1}$$

where ρ_c is the conditional density matrix, dW is the Wiener increment, and individual realizations of the measurement current obey the differential equation

$$dD = \gamma(\langle A\rangle_c - D)dt + \frac{\gamma}{\sqrt{4\lambda}}dW, \tag{A2}$$

with $\langle A\rangle_c = \mathrm{Tr}(A\rho_c)$. The stochastic unraveling provides a direct connection with experiments and also allows for maximum flexibility, since one can implement any kind of feedback protocol desired: One simply modifies the Liouvillian $\mathcal{L}(D)$ to have any desired dependence on D; in a single stochastic trajectory, the obtained value of D at each step is then simply input back into Eq. (A1). One can draw a direct analogy with the comparison between the Langevin equation and the Fokker-Planck equation in classical Brownian motion. Both equations describe the same physical phenomena, but from different angles, and therefore both have their uses.

We illustrate how stochastic trajectories compare with the deterministic equation (3) through the lenses of a specific example, namely, the same driven qubit example as in the main text (cf. Fig. 1). In Fig. 8 we show how the average, variance, and covariance change in time for this process using both stochastic trajectories (blue) and Fokker-Planck equation solutions (orange). As noted in the main text, the steady-state values for these parameters are exactly determined by our method to be $\langle D\rangle = 0$, $\mathrm{Var}(D) = 1.1$, and $\mathrm{Cov}(\sigma_z, D) = 0.6$ (gray horizontal line). Note that while the first two quantities only depend on the statistics of the measurement current, the final quantity also depends on the conditional state. The solution method proposed in the main text is particularly convenient for this problem, as it only required $N = 5$ matrices in Eq. (4). Moreover, our method goes directly to the steady state, i.e., it does not require simulating transient effects, which is always necessary with stochastic trajectories. Figure 9 illustrate the steady-state mean and variance for different numbers of stochastic realizations. This provides an idea of how many samples are needed to reach convergence, although the precise value of course is problem specific.

APPENDIX B: INFORMATIONAL QUANTITIES

In the following, we outline some useful informational quantities that can be computed from the joint state.

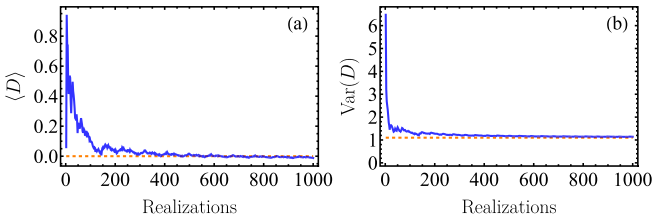

FIG. 9. Steady-state value of (a) the mean $\langle D\rangle$ and (b) the variance $\mathrm{Var}(D)$ against the number of stochastic realizations used (blue solid line). Exact steady-state values are shown by orange dashed lines and the other parameters are the same as in Fig. 1.

1. Mutual information between system and detector

We consider the mutual information between the system and detector. This can be expressed as

$$\mathcal{I} = S\left[\int dD\rho_t(D)\right] + S[\mathrm{Tr}[\rho_t(D)]] - S[\rho_t(D)], \quad \text{(B1)}$$

where $S[\cdot]$ is either the von Neumann or Shannon entropy, depending on the input. We simplify each term separately. The first part is simply

$$S\left[\int dD\,\rho_t(D)\right] = S[M_0] \quad \text{(B2)}$$

$$= -\mathrm{Tr}M_0 \ln M_0. \quad \text{(B3)}$$

The second term can be expanded as

$$S[\mathrm{Tr}[\rho_t(D)]] = S[P(D)] \quad \text{(B4)}$$

$$= -\int dD\,P(D)\ln P(D). \quad \text{(B5)}$$

The final term is then

$$S[\rho_t(D)] = -\int dD\,\mathrm{Tr}[\rho_t(D)\ln\rho_t(D)]. \quad \text{(B6)}$$

By defining the density matrix given the outcome D as $\tilde{\rho}_t(D) = \rho_t(D)/P(D)$ one can show that the mutual information is equivalent to

$$\mathcal{I} = -\int dD\,S[\tilde{\rho}_t(D)]P(D) + S[M_0]. \quad \text{(B7)}$$

For a Hilbert space of dimension R, the maximum of this mutual information is then $\ln R$.

2. Correlation

If an observable has a spectral decomposition $B = \sum_n b_n|b_n\rangle\langle b_n|$, then there is a joint probability distribution $P(b_n, D) = \langle b_n|\rho(D)|b_n\rangle$. One can then ask about the covariance of this distribution.

The expected measurement outcome is given by

$$\langle D\rangle = \int dD\,D\,P(D) \quad \text{(B8)}$$

$$= \sqrt{\sigma}c_1. \quad \text{(B9)}$$

Similarly, we have that, for B, the unconditional expectation is

$$\langle B\rangle = \mathrm{Tr}(M_0B). \quad \text{(B10)}$$

We define the covariance as

$$\mathrm{cov}(B, D) = \mathrm{Tr}\int dD\,B\,D\,\rho(D) - \langle D\rangle\cdot\langle B\rangle \quad \text{(B11)}$$

$$= \sqrt{\sigma}\mathrm{Tr}(M_1B) - \sqrt{\sigma}c_1\mathrm{Tr}(M_0B) \quad \text{(B12)}$$

$$= \sqrt{\sigma}[\mathrm{Tr}(M_1B) - \mathrm{Tr}(M_1)\mathrm{Tr}(M_0B)]. \quad \text{(B13)}$$

This follows from the identity

$$\int dD\,D\frac{\mathcal{H}_n(D)}{\sqrt{\sigma^n n!}}\frac{e^{-D^2/2\sigma}}{\sqrt{2\pi\sigma}} = J_n(1) \quad \text{(B14)}$$

$$= \sqrt{\sigma(n+1)}\delta_{n+1,0} + \sqrt{n\sigma}\delta_{n-1,0} \quad \text{(B15)}$$

$$= \sqrt{n\sigma}\delta_{n-1,0}, \quad \text{(B16)}$$

since $n \geqslant 0$. Note that $\mathrm{Cov}(B)$ is identically zero if $M_1 = 0$, which is the case for a product state between the system and detector.

APPENDIX C: TWO-TIME CORRELATION OF FILTERED OUTPUT CURRENT

We want to compute $\langle D(t)D(s)\rangle$, which is explicitly given by

$$\langle D(t)D(s)\rangle = \int_{-\infty}^{t}\int_{-\infty}^{s} dt_2dt_1\gamma^2e^{-\gamma(t-t_2+s-t_1)}\langle z(t_1)z(t_2)\rangle. \quad \text{(C1)}$$

The expression for the term inside the integral is given in steady state by [1]

$$\langle z(t)z(t+t')\rangle = \frac{1}{4\lambda}\delta(t') + \frac{1}{4}\mathrm{Tr}(\mathcal{C}_Ae^{\Lambda t'}\mathcal{C}_AM_0) \quad \text{(C2)}$$

$$= \frac{1}{4\lambda}\delta(t') + \mathrm{Tr}(AM_0)^2 + \frac{1}{2}\sum_{j\neq0}e^{\eta_jt'}\mathrm{Tr}(Ax_j)\mathrm{Tr}(y_j^\dagger\{A, M_0\}), \quad \text{(C3)}$$

where we have used the spectral decomposition of Λ and assumed no feedback. The end result is

$$\langle D(t+\tau)D(t)\rangle = \gamma^2\int_{-\infty}^{t+\tau}\int_{-\infty}^{t} dt_2dt_1e^{-\gamma(2t+\tau-t_2-t_1)}\left(\frac{1}{4\lambda}\delta(t_2-t_1) + \mathrm{Tr}(AM_0)^2 + \frac{1}{2}\sum_{j\neq0}e^{\eta_j|t_2-t_1|}\mathrm{Tr}(Ax_j)\mathrm{Tr}(y_j^\dagger\{A, M_0\})\right) \quad \text{(C4)}$$

$$= \sigma e^{-\gamma\tau} + \mathrm{Tr}(AM_0)^2 + \frac{1}{2}\sum_{j\neq0}\frac{\gamma(\gamma e^{\tau\eta_j} + e^{-\gamma\tau}\eta_j)}{\gamma^2-\eta_j^2}\mathrm{Tr}(Ax_j)\mathrm{Tr}(y_j^\dagger\{A, M_0\}). \quad \text{(C5)}$$

The $\tau = 0$ case matches the result from the methods in the main text. Since the average filtered detector outcome in steady state is $\langle D\rangle = \mathrm{Tr}(AM_0)$, we can write our final result as

$$C(\tau) = \langle D(t+\tau)D(t)\rangle - \langle D(t)\rangle^2 \tag{C6}$$

$$= \sigma e^{-\gamma\tau} + \frac{1}{2}\sum_{j\neq 0}\frac{\gamma(\gamma e^{\tau\eta_j} + e^{-\gamma\tau}\eta_j)}{\gamma^2 - \eta_j^2}$$

$$\mathrm{Tr}(Ax_j)\mathrm{Tr}(y_j^\dagger\{A, M_0\}). \tag{C7}$$

APPENDIX D: FOKKER-PLANCK EQUATION IN HERMITE POLYNOMIAL BASIS

Since it will frequently arise, we note the orthogonality relation

$$\int_{-\infty}^{\infty}\frac{\mathcal{H}_m(x)}{\sqrt{\sigma^m m!}}\frac{\mathcal{H}_n(x)}{\sqrt{\sigma^n n!}}\frac{e^{-x^2/2\sigma}}{\sqrt{2\pi\sigma}}dx = \delta_{n,m}. \tag{D1}$$

We start with the normalization condition that $\int_{-\infty}^{\infty} dD\,\mathrm{Tr}[\rho_t(D)] = 1$. Using the orthogonality relation, we can write this as

$$\int_{-\infty}^{\infty} dD\,\mathrm{Tr}[\rho_t(D)] = \sum_{n=0}^{N-1}\mathrm{Tr}(M_n)\int_{-\infty}^{\infty} dD\frac{\mathcal{H}_n(D)}{\sqrt{\sigma^n n!}}\frac{e^{-D^2/2\sigma}}{\sqrt{2\pi\sigma}} \tag{D2}$$

$$= \sum_{n=0}^{N-1}\mathrm{Tr}(M_n)\delta_{n,0} \tag{D3}$$

$$= \mathrm{Tr}(M_0). \tag{D4}$$

So the normalization condition simplifies to $\mathrm{Tr}(M_0) = 1$, where $\int dD\,\rho_t(D) = \sum_n M_n\delta_{n,0} = M_0$ describes the state of the system when ignorant of the measurement outcome.

We now move on to the main equation. Our strategy will be to insert our ansatz for the state (4) into Eq. (3) and compute each term by applying $\int_{-\infty}^{\infty} dD\,\mathcal{H}_m(D)/\sqrt{\sigma^m m!}$ and utilizing the orthogonality relation (this is often indicated by an arrow).

We start with the time derivative which only acts on the M_n matrices, leading to $\sum_{n=0}^{N-1}\dot{M}_n\delta_{n,m} = \dot{M}_m$. Next we will consider the first term on the right-hand side of Eq. (3). This is the outcome-dependent Lindblad operator $\mathcal{L}(D)$. This gives

$$\sum_{n=0}^{N-1}\int_{-\infty}^{\infty} dD\frac{\mathcal{H}_m(D)}{\sqrt{\sigma^m m!}}\frac{\mathcal{H}_n(D)}{\sqrt{\sigma^n n!}}\frac{e^{-D^2/2\sigma}}{\sqrt{2\pi\sigma}}\mathcal{L}(D)M_n. \tag{D5}$$

We write this in full generality as $\mathcal{L}(D) = \mathcal{L}_0 + \sum_p f_p(D)\mathcal{L}_p$. Altogether then Eq. (D5) simplifies to $\mathcal{L}_0 M_m + \sum_{n=0}^{N-1}\sum_p \alpha_{n,m,p}\mathcal{L}_p M_n$, where

$$\alpha_{n,m,p}(t) = \int_{-\infty}^{\infty} dD\frac{\mathcal{H}_m(D)}{\sqrt{\sigma^m m!}}\frac{\mathcal{H}_n(D)}{\sqrt{\sigma^n n!}}\frac{e^{-D^2/2\sigma}}{\sqrt{2\pi\sigma}}f_p(D). \tag{D6}$$

Moving on to the measurement backaction term, it simplifies as $-\frac{\lambda}{2}\sum_{n=0}^{N-1}[A,[A,M_n]]\delta_{n,m} = -\frac{\lambda}{2}[A,[A,M_m]]$, where $[\cdot,\cdot]$ is the commutator. The penultimate term in Eq. (3) (describing the overall drift) is given by

$$-\gamma\,\partial_D\mathcal{C}_{A-D}\rho_t(D)/2 = -\frac{\gamma}{2}\partial_D\{A - D,\,\rho_t(D)\} \tag{D7}$$

$$= -\frac{\gamma}{2}[\{-1,\,\rho_t(D)\} + \{A - D,\,\partial_D\rho_t(D)\}], \tag{D8}$$

where we write the identity as 1. In order to evaluate $\partial_D\rho_t(D)$, we note that

$$\partial_D\big[\mathcal{H}_n(D)e^{-D^2/2\sigma}\big] = -e^{-D^2/2\sigma}\sigma^{-1}\mathcal{H}_{n+1}(D). \tag{D9}$$

Inserting the ansatz (4) and applying $\int_{-\infty}^{\infty} dD\,\mathcal{H}_m(D)/\sqrt{\sigma^m m!}$, the drift term can be evaluated in separate parts as

$$\{-1,\,\rho_t(D)\} \to \sum_n\{-1, M_n\}\delta_{n,m} \tag{D10}$$

$$= \{-1, M_m\} \tag{D11}$$

$$= -2M_m \tag{D12}$$

and

$$\{A,\,\partial_D\rho_t(D)\} \to -\sigma^{-1}\sum_n\{A, M_n\}\delta_{n+1,m}\sqrt{(n+1)\sigma} \tag{D13}$$

$$= -\sqrt{\frac{m}{\sigma}}\{A, M_{m-1}\}. \tag{D14}$$

For the final part, we will exploit the shift rule that $x\mathcal{H}_n(x) = \mathcal{H}_{n+1}(x) + n\sigma\mathcal{H}_{n-1}(x)$. The last part is then

$$\{-D,\,\partial_D\rho_t(D)\} = -2D\partial_D\rho_t(D) \tag{D15}$$

$$= 2D\sigma^{-1}\sum_n M_n\frac{\mathcal{H}_{n+1}(D)}{\sqrt{\sigma^n n!}}\frac{e^{-D^2/2\sigma}}{\sqrt{2\pi\sigma}} \tag{D16}$$

$$= 2\sigma^{-1}\sum_n M_n\frac{1}{\sqrt{\sigma^n n!}}\frac{e^{-D^2/2\sigma}}{\sqrt{2\pi\sigma}}[\mathcal{H}_{n+2}(D) + (n+1)\sigma\mathcal{H}_n(D)] \tag{D17}$$

$$\to 2\sigma^{-1}\sum_n M_n[\delta_{n+2,m}\sqrt{(n+2)(n+1)}\sigma + (n+1)\sigma\delta_{n,m}] \tag{D18}$$

$$= 2[\sqrt{m(m-1)}M_{m-2} + (m+1)M_m]. \tag{D19}$$

Finally, we tackle the very last term in Eq. (3), which can be thought of as a diffusion. It can then be expressed as

$$\frac{\gamma^2}{8\lambda}\partial_D^2\rho_t(D) \to \frac{\gamma^2}{8\lambda}\frac{1}{\sigma^2}\sum_n M_n\delta_{n+2,m}\sqrt{(n+2)(n+1)}\sigma \tag{D20}$$

$$= \frac{\gamma^2}{8\lambda}\frac{\sqrt{m(m-1)}}{\sigma}M_{m-2} \tag{D21}$$

$$= \gamma\sqrt{m(m-1)}M_{m-2}. \tag{D22}$$

In summary, the equation can then be written as the coupled differential equation

$$\dot{M}_m = \mathcal{L}_0 M_m + \sum_{n=0}^{N-1}\sum_p \alpha_{n,m,p}\mathcal{L}_p M_n - \frac{\lambda}{2}[A,[A,M_m]] - \frac{\gamma}{2}\left(2mM_m - \sqrt{\frac{m}{\sigma}}\{A,M_{m-1}\}\right) \tag{D23}$$

for each m with the normalization condition $\mathrm{Tr}(M_0) = 1$. Note that $M_{-1} = 0$.

APPENDIX E: MATRIX COEFFICIENTS FOR POLYNOMIAL FEEDBACK

We wish to compute the coefficients $\alpha_{n,m,p}$ for a polynomial feedback function $f_p(D) = D^p$. This can be computed by noting that $\alpha_{n,m,0} = \delta_{n,m}$ and the recursive relation for this case

$$\alpha_{n,m,p} = \sqrt{\sigma(m+1)}\alpha_{n,m+1,p-1} + \sqrt{\sigma m}\alpha_{n,m-1,p-1}. \tag{E1}$$

For example, the quadratic case is

$$\alpha_{n,m,2} = \sigma\sqrt{(m+1)(n+1)}\delta_{m+1,n+1} + \sigma\sqrt{n(m+1)}\delta_{m+1,n-1} + \sigma\sqrt{m(n+1)}\delta_{n+1,m-1} + \sigma\sqrt{nm}\delta_{n-1,m-1}. \tag{E2}$$

[1] G. T. Landi, M. J. Kewming, M. T. Mitchison, and P. P. Potts, Current fluctuations in open quantum systems: Bridging the gap between quantum continuous measurements and full counting statistics, PRX Quantum **5**, 020201 (2024).

[2] S. Gleyzes, S. Kuhr, C. Guerlin, J. Bernu, S. Deleglise, U. B. Hoff, M. Brune, J. M. Raimond, and S. Haroche, Quantum jumps of light recording the birth and death of a photon in a cavity, Nature (London) **446**, 297 (2007).

[3] S. Gustavsson, R. Leturcq, B. Simovič, R. Schleser, T. Ihn, P. Studerus, K. Ensslin, D. C. Driscoll, and A. C. Gossard, Counting statistics of single electron transport in a quantum dot, Phys. Rev. Lett. **96**, 076605 (2006).

[4] J. C. Bayer, F. Brange, A. Schmidt, T. Wagner, E. P. Rugeramigabo, C. Flindt, and R. J. Haug, Real-time detection and control of correlated charge tunneling in a quantum dot, Phys. Rev. Lett. **134**, 046303 (2025).

[5] R. Vijay, D. H. Slichter, and I. Siddiqi, Observation of quantum jumps in a superconducting artificial atom, Phys. Rev. Lett. **106**, 110502 (2011).

[6] K. W. Murch, S. J. Weber, C. Macklin, and I. Siddiqi, Observing single quantum trajectories of a superconducting quantum bit, Nature (London) **502**, 211 (2013).

[7] Z. K. Minev, S. O. Mundhada, S. Shankar, P. Reinhold, R. Gutiérrez-Jáuregui, R. J. Schoelkopf, M. Mirrahimi, H. J. Carmichael, and M. H. Devoret, To catch and reverse a quantum jump mid-flight, Nature (London) **570**, 200 (2019).

[8] H. M. Wiseman and G. J. Milburn, *Quantum Measurement and Control* (Cambridge University Press, New York, 2009).

[9] M. J. Kewming, A. Kiely, S. Campbell, and G. T. Landi, First passage times for continuous quantum measurement currents, Phys. Rev. A **109**, L050202 (2024).

[10] B. Annby-Andersson, F. Bakhshinezhad, D. Bhattacharyya, G. De Sousa, C. Jarzynski, P. Samuelsson, and P. P. Potts, Quantum Fokker-Planck master equation for continuous feedback control, Phys. Rev. Lett. **129**, 050401 (2022).

[11] G. F. Diotallevi, B. Annby-Andersson, P. Samuelsson, A. Tavakoli, and P. Bakhshinezhad, Steady-state entanglement production in a quantum thermal machine with continuous feedback control, New J. Phys. **26**, 053005 (2024).

[12] G. De Sousa, P. Bakhshinezhad, B. Annby-Andersson, P. Samuelsson, P. P. Potts, and C. Jarzynski, Continuous feedback protocols for cooling and trapping a quantum harmonic oscillator, Phys. Rev. E **111**, 014152 (2025).

[13] B. Annby-Andersson, D. Bhattacharyya, P. Bakhshinezhad, D. Holst, G. De Sousa, C. Jarzynski, P. Samuelsson, and P. P. Potts, Maxwell's demon across the quantum-to-classical transition, Phys. Rev. Res. **6**, 043216 (2024).

[14] M. M. Wolf, F. Verstraete, M. B. Hastings, and J. I. Cirac, Area laws in quantum systems: Mutual information and correlations, Phys. Rev. Lett. **100**, 070502 (2008).

[15] H. Cramér, *Mathematical Methods of Statistics* (Princeton University Press, Princeton, 1946).

[16] C. R. Rao, Bull. Calcutta Math. Soc. **37**, 81 (1945).

[17] J. A. Smiga, M. Radaelli, F. C. Binder, and G. T. Landi, Stochastic metrology and the empirical distribution, Phys. Rev. Res. **5**, 033150 (2023).

[18] P. Facchi and S. Pascazio, Quantum Zeno dynamics: Mathematical and physical aspects, J. Phys. A: Math. Theor. **41**, 493001 (2008).

[19] K. Prech, J. Aschwanden, and P. P. Potts, Quantum thermodynamics of continuous feedback control, arXiv:2505.16615.

[20] C. Elouard, D. Herrera-Martí, B. Huard, and A. Auffèves, Extracting work from quantum measurement in Maxwell's demon engines, Phys. Rev. Lett. **118**, 260603 (2017).

[21] D. Guéry-Odelin, A. Ruschhaupt, A. Kiely, E. Torrontegui, S. Martínez-Garaot, and J. G. Muga, Shortcuts to adiabaticity: Concepts, methods, and applications, Rev. Mod. Phys. **91**, 045001 (2019).

[22] C. P. Koch, Controlling open quantum systems: Tools, achievements, and limitations, J. Phys.: Condens. Matter **28**, 213001 (2016).

[23] M. H. Goerz, D. Basilewitsch, F. Gago-Encinas, M. G. Krauss, K. P. Horn, D. M. Reich, and C. P. Koch, Krotov: A Python implementation of Krotov's method for quantum optimal control, SciPost Phys. **7**, 080 (2019).

[24] S. Borah, B. Sarma, M. Kewming, G. J. Milburn, and J. Twamley, Measurement-based feedback quantum control with deep reinforcement learning for a double-well nonlinear potential, Phys. Rev. Lett. **127**, 190403 (2021).

[25] R. Porotti, A. Essig, B. Huard, and F. Marquardt, Deep reinforcement learning for quantum state preparation with weak nonlinear measurements, Quantum **6**, 747 (2022).

[26] C. Whitty, A. Kiely, and A. Ruschhaupt, Quantum control via enhanced shortcuts to adiabaticity, Phys. Rev. Res. **2**, 023360 (2020).